Letter Vol. 43, No. 4 / 15 February 2018 / Optics Letters 847

Ultralow-threshold continuous-wave lasing assisted by a metallic optofluidic cavity exploiting continuous pump

Hailang Dai,[1,2,†] Bei Jiang,[1,2,†] Cheng Yin,[1,3] Zhuangqi Cao,[1] and Xianfeng Chen[1,2,*]

[1]The State Key Laboratory on Fiber Optic Local Area Communication Networks and Advanced Optical Communication Systems, Department of Physics and Astronomy, Shanghai JiaoTong University, Shanghai 200240, China
[2]Collaborative Innovation Center of IFSA (CICIFSA), Shanghai Jiao Tong University, Shanghai 200240, China
[3]Jiangsu Key Laboratory of Power Transmission and Distribution Equipment Technology, Hohai University, Changzhou 213022, China
*Corresponding author: xfchen@sjtu.edu.cn

Received 1 December 2017; revised 10 January 2018; accepted 10 January 2018; posted 16 January 2018 (Doc. ID 314790); published 12 February 2018

We report an ultralow-threshold continuous-wave lasing via a metallic optofluidic resonant cavity based on the symmetrical metal-cladding waveguide. The high quality factor Q and spontaneous emission coupling factor β of the waveguide strengthen the interaction between the gain medium and the ultrahigh order modes (UOMs); hence, the room-temperature, narrowband lasing can be effectively pumped by a continuous laser of low intensity. Rhodamine 6G and methylene blue are chosen to verify the applicability of the proposed concept. Lasing is emitted from the chip surface when the pumped laser is well coupled into the UOMs. For methylene blue with a concentration of $2.57 * 10^{-13}$ mol/ml, the operated emission can be observed with the launched pump threshold as low as $2.1\ \mu W/cm^2$.

OCIS codes: (140.0140) Lasers and laser optics; (140.2050) Dye lasers; (140.3410) Laser resonators; (140.3945) Microcavities; (230.3990) Micro-optical devices.

https://doi.org/10.1364/OL.43.000847

Optical microcavities, which confine the resonant modes to very small volumes, figure prominently in research fields such as optics and solid-state physics [1]. Combining the small cavity volume and high Q-factor, the microcavity is believed to be most promising for the pursuit of efficient and compact light source with low power dissipation and fast modulation speed [2]. Particularly, microcavity, or even nanocavity, lasers are taking on increased importance. For illustration, lasing based on whispering gallery microcavities [3], droplets [4], semiconductor cavities [5], organic dye lasers [6,7], and photonic-crystal nanocavities or quantum dots [8] are already demonstrated due to the remarkable progress in the fabrication process. Among these, low-threshold or thresholdless lasing is of particular interest. In the weak coupling regime, the spontaneous emission rate is enhanced compared to the no cavity case, i.e., a quantum optical effect known as the Purcell effect [9,10]. The enhancement factor is presented by $3\lambda^3 Q/4\pi^2 n^3 V$; thus, the extreme confinement of the electric field by the small microcavity volume is essential for the observation of the Purcell effect. On the other hand, the spontaneous emission coupling factor β is also proportional to the inverse of the mode volume, i.e., the microcavity volume [11]. As β increases, the pump threshold behavior gradually disappears and, towards the limit of $\beta = 1$, a thresholdless laser is theoretically possible [12]. Generally, the design of microlasers falls into two categories: one refers to the case when the bandwidth of the cavity mode is much wider than that of the gain medium. In R6G, for an, extremely small cavity is required since the gain medium has a broad bandwidth of 50 nm. Few structures are eligible for this case, including InGaN microdisks on silicon [13], vertical cavity surface-emitting lasers [14], and WSe2–cavity systems [15]. In contrast, Rabi oscillation [16] and one-atom laser operation belong to the second category, where the cavity resonance peak is sharper than the gain bandwidth, leading to coherent effects. In both cases, high power pumping and high concentrations of a dye medium are indispensable. However, high pump power can destroy the dye molecule structure, while a high concentration of the active solution can increase collision probability and result in fluorescent quenching. The application as a laser dye of methylene blue is significantly limited due to the fluorescent quenching. Despite the above mentioned difficulties, microcavity or nanocavity structures are still most favored and widely pursued in the design of ultralow-threshold compact laser.

Different from the usual choice of subwavelength cavities, this Letter adopts a "macroscale" optofluidic waveguide cavity and demonstrates narrowband lasing peaks. Instead of the directional output of a conventional laser, our waveguide structure dictates concentric-cone-like emission in the vertical direction of its surface. We will demonstrate that the pump threshold can be significantly reduced in the resonant cavity whose dimension is far beyond the wavelength scale, if the specific symmetrical metal-cladding waveguide (SMCW) structure

is introduced to enhance the interaction between the gain medium and the resonant modes. This waveguide chip includes a millimeter thick resonant cavity filled with an active medium, which is possible to host thousands of guided modes. Among them, the ultrahigh order modes (UOMs) excited at small incident angle are especially important; its standing optical field oscillates rapidly between the metallic coupling layer and substrate, resulting in various interesting properties, such as strong field enhancement effect, high sensitivity, and polarization independence. These attributes motivate much of the research on this structure, including precision metrology [17], biosensing [18], and integrated optical components [19]. The recent discovered intermode coupling effect, which is demonstrated by a series of reflection cones, reveals the intrinsic energy shift between the adjacent modes [20]. In this Letter, methylene blue of low concentration was also adopted as an active medium to reduce its fluorescent quenching effect. Exploiting a continuous laser as the pump, the experimental threshold intensity of methylene blue with a concentration of $2.57 * 10^{-13}$ mol/ml is merely 2.1 $\mu W/cm^2$. This demonstrates the potential application of the SMCW structure as a low-threshold coherent source, which fully benefits from the excellent optical parallelism. Our chip is easy to produce at low cost and may open new avenues for lab-on chip or optofluidics integration.

The SMCW structure includes an upper coupling metal layer, a thick metal substrate and a millimeter scale guiding layer. The metal claddings are symmetric, and the resonant cavity is different from the conventional Fabry–Perot resonator in many aspects. For example, the effective index of the guided modes can approach zero, independent of the specific design of the guiding layer. In contrast to the case reported in [21], no propagating plasmon wave is involved in our devices, since direct coupling from the free space without a high-index prism is applied, as is shown in Fig. 1(b). In the guiding layer, the resonant modes oscillate with high intensity due to the field enhancement effect, and the numerical simulations verify that the Poynting vector of the modes can be enhanced 60 times more than the incident light [22]. Thus, the mode density for photons in the resonant UOM is high. Since the guiding layer is three orders of magnitude larger than the wavelength, the transversal wave vector difference between two adjacent modes is small due to the high mode density, which yields the physics behind intermode coupling. On the other hand, the FWHM of each resonant dip is extremely small, leading to the high Q-factor. The theoretical prediction of the Q-factor is of 10^4 orders. Besides the high Q-factor, the β value of our waveguide chip structure is also high, despite the usual intuition that a microcavity is indispensable to obtaining high β. With increasing β, the threshold in the pump intensity gradually decreases until a thresholdless laser is achieved in the $\beta = 1$ limit, which corresponds to a closed cavity. For our SMCW structure, the mode volume is not equal to the cavity volume, so we calculate the volume of the guided mode analytically, and a simple expression for β is proposed. For a concrete example of a simplified three-layered model, numerical simulations are carried out to calculate the β value for different mode orders m. The parameters are as follows: the wavelength is 473 nm, the dielectric constant of the silver is $\varepsilon_{Ag} = -8.4 + 0.23i$, the thickness of the coupling layer is 45 nm, and the thickness of the guiding layer is $d = 1$ mm with a dielectric constant $\varepsilon_1 = 1.33^2$. For $m = 3373$, the effective index of the mode is $N \approx 1.064 + 2.492 * 10^{-7} i$, and the β value is found to be 0.1461. For $m = 4479$, the effective index is $N \approx 0.7007 + 7.797 * 10^{-7} i$, and the β value equals to 0.1455. For comparison, the β value for a plane mirror Fabry–Perot configuration is about 0.1. It is interesting to note that the β value does not vary much as the mode order changes, and its high value guarantees that our structure would greatly reduce the threshold. Let us discuss briefly the physics behind the reflection cones [Fig. 2(a)], which are intimately related with the mechanism of how the amplified coherent light is emitted from the resonant cavity of the waveguide chip. When the incident laser reaches the chip surface, its energy is coupled and stored in the guided layer as guided modes. Since the upper metallic layer is thin, all these UOMs are leaky modes. For a specific UOM with a fixed transverse wave number, a concentric light cone can be observed, as its energy converts back to freely propagating light though the leakage radiation from the coupling layer. This is different from the specular reflection, which produces only a bright spot on the screen. Intuitively, a collimated laser beam can only excite one UOM with the same transverse wave vector. However, the experimental results reveal a series of

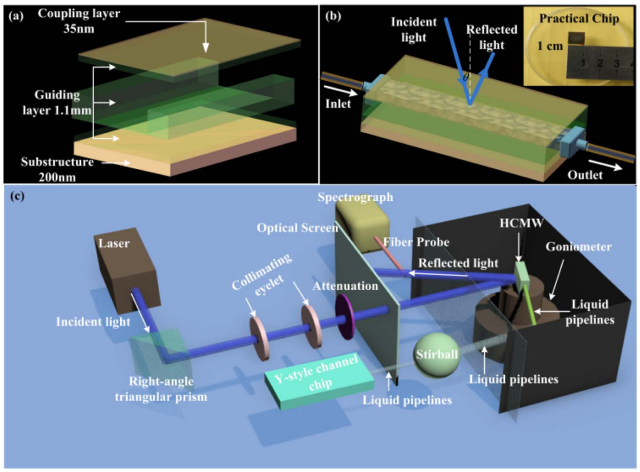

Fig. 1. Structure of a SMCW chip and the experimental setup. (a) Schematic diagram of the SMCW chip. The thickness of the coupling layer ranges from 30 to 50 nm, and the metal substrate is about 300 nm. The guiding layer which contains a channel is 1.1 mm thick. (b) Excitation of UOMs via a free space coupling technique. Inset: the photo of the waveguide chip. (c) Schematic of the experimental setup.

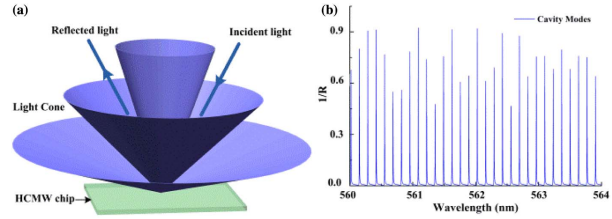

Fig. 2. Theory of SMCW and cavity modes in cavity. (a) Schematic diagram of the reflected light cones formed by leakage radiation of the UOMs, while the reflection law generates the specular reflected beam. (b) Spectrum of cavity modes ranging from 560 to 564 nm of a specific waveguide structure. The parameters are that the dielectric constant of silver is $\varepsilon_{Ag} = -13.53 + 0.42i$, and the guiding layer is 1 mm thick and with $\varepsilon = 2.3007$.

reflection cones, while each cone corresponds to a specific UOM. Intuitively, a collimated laser beam can only excite one UOM with the same transverse wave vector. However, the experimental results reveal a series of reflection cones, while each cone corresponds to a specific UOM. The physics behind the results can be explained as follows: after the incident energy was coupled and stored in the guiding layer, the leakage radiation can take place via all the UOM channels, while each mode leakage produces a reflection cone. The emission process of the coherent light through the resonant cavity is very similar, so a series of concentric cones of different wavelength can be observed experimentally.

Experiments are carried out to verify the above hypothesis. The experimental setup [Fig. 1(c)] is similar to the one we used to observe the reflection cones, except the dye solution, i.e., the gain medium, is injected into the SMCW chip. A diode pumped solid state CW laser of 15 mW with a wavelength of 473 nm is used as the pump, while the wavelength is chosen for better absorption of the methylene blue. Output emission is collected with an optical fiber and sent to a spectrometer to measure the wavelength of the coherent light emission. In order to investigate the relation between light emission and UOM coupling, a PC-controlled $\theta/2\theta$ goniometer is applied to adjust the incident angle. An attenuator (GCM-09) was placed in the optical path to control the laser intensity. A beam splitter was used to divide the light beam into two parts, while one part was measured by an optical power meter (COHERENT FM 33-0506). The concentrations of active solutions R6G and methylene blue are $3.615 * 10^{-13}$ mol/ml and $2.579 * 10^{-13}$ mol/ml, respectively. As shown in Fig. 3, coherent light emission of 570 nm was observed in the first illustration via an R6G laser dye whose fluorescence spectra range from 550 to 600 nm. The image on the screen shows the existence of another series of red cones corresponding to the coherent laser emission [Fig. 3(a)], whose emission process is similar to the UOM leakage process, i.e., the energy converts back to free space via all the UOM channels. In the Figs. 3(a) and 3(b), a transverse shift in the incident plane is discernable between the blue cones' axes and the red cones' axes. This implies that the center of the coherent light emission is slightly shifted in the guiding layer from the center of the UOMs excited by the incidence.

The second experiment used methylene blue as gain medium to study the relation between the coupling condition and the lasing characteristics. Photoluminescence is performed at various incident angles to tune the coherent light excitation with respect to the UOM coupling efficiency. As shown in Figs. 4(b)–4(d), two emission peaks of very narrow bandwidth via methylene blue can be observed at the wavelength of 708.5 and 723.1 nm, respectively. By adjusting the incident angle, it is found that the intensity of both the fluorescence and light emission depends crucially on the coupling efficiency of the UOMs. In the case of best coupling ($\theta = 5.6°$), the output intensity is high while, at a very poor coupling condition ($\theta = 6.2°$), the light emission is almost indiscernible.

Measured at the optimized coupling condition of the UOMs, the emission threshold behavior was also studied by attenuating the pump intensity, while the other experimental parameters remain unvaried. Figure 5 shows the measured output intensity as a function of excitation pump density. It is shown that the lasing pump threshold for methylene blue is as low as 2.1 $\mu W/cm^2$. A detailed calculation of coupling efficiency of lasing is shown in Table 1.

Different from the usual strategy of using microcavity or nanocavity structure, a novel low-threshold dye lasing based on a millimeter scale resonant cavity was proposed. Taking advantage of the high Q and β value of the SMCW structure, the experimental threshold was significantly reduced; a continuous laser pump and active solution of extremely low concentration are sufficient at room temperature. The coherent light emission results in a series of concentric lasing cones, which is similar to the leakage radiation of the UOMs. The output cones undergo a transverse shift to the UOM leakage cones. In addition to an

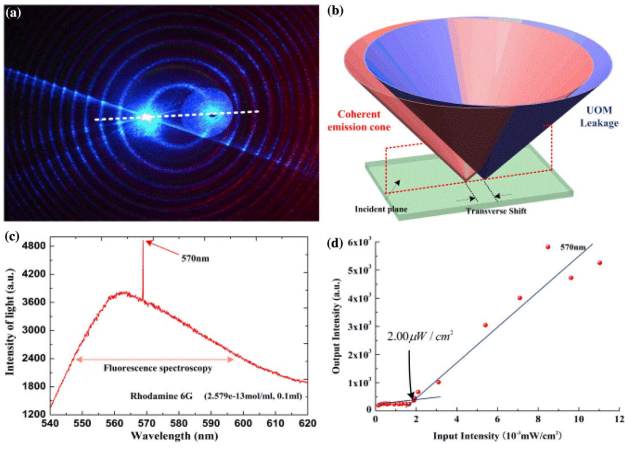

Fig. 3. Experimental result of the R6G dye laser. (a) Image of the concentric laser cones (red) and the leakage cones of the UOMs (blue) on the screen, where the white dashed line connects the incident (right) and reflected (left) light spots. (b) Schematic of a specific laser cone and a specific leakage cone of an UOM. (c) Emission spectrum of the R6G sample, where the lasing wavelength is 570 nm. (d) Threshold behavior of the dye laser of R6G, where the lasing threshold is around 2.0 $\mu W/cm^2$.

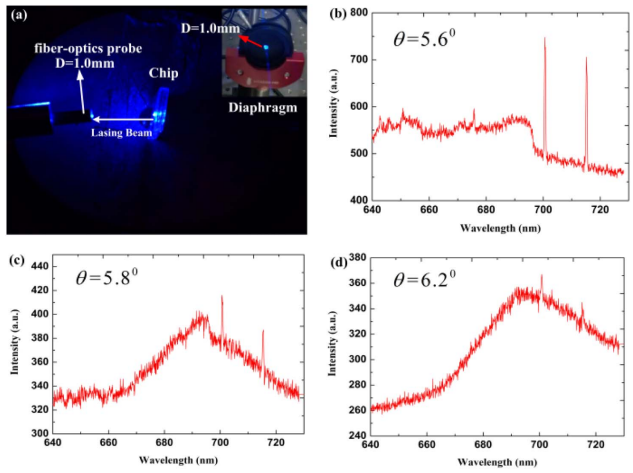

Fig. 4. (a) Fiber-optics probe of the spectrometer and the SMCW chip are fixed on the $\theta/2\theta$ goniometer, whose rotation is controlled by the PC. Inset: the cross section of the probe. (b)–(d) Emission spectrum of the methylene blue at different incident angles, i.e., different coupling efficiencies of the UOMs. The incident angles are 5.6°, 5.8°, and 6.2°, respectively.

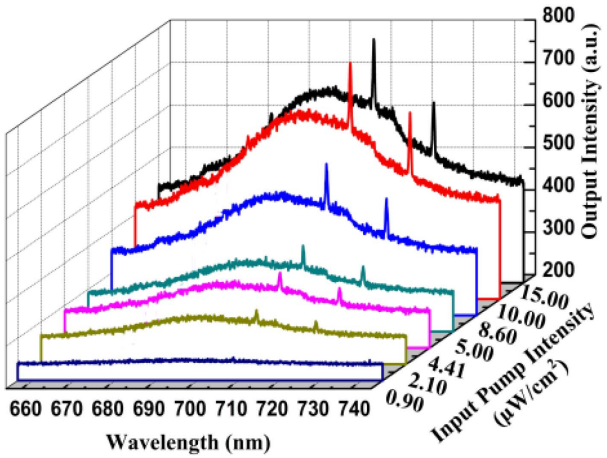

Fig. 5. Threshold behavior of a methylene blue dye laser.

Table 1. Calculated Results of Lasing Efficiency of Methylene Blue

The intensity of input pumping ($\mu W/cm^2$)								
I_{input}	1.6	1.8	2.0	2.2	2.4	2.6	2.8	3.0
The intensity of output lasing peaks ($\mu W/cm^2$)								
I_{output}	0.021	0.023	0.028	0.030	0.035	0.039	0.045	0.048
The lasing efficiency of this process $\beta = I_{output}/I_{input}(\%)$								
β	1.31	1.28	1.40	1.36	1.45	1.50	1.64	1.54

easy fabrication process, effective modulation can be achieved by adjusting the coupling efficiency of UOMs. Given the attributes mentioned above, our "macroscale" optofluidic resonant cavity structure may open up new prospects for many fields such as optofluidics and biosensors.

Funding. National Basic Research Programmer of China (2013CBA01703); National Natural Science Foundation of China (NSFC) (11404092, 61265001, 61405117; 11764020); China Postdoctoral Science Foundation (2016M601586).

†These authors contributed equally to this Letter.

REFERENCES

1. K. J. Vahala, Nature **424**, 839 (2003).
2. C. Walther, G. Scalari, M. I. Amanti, M. Beck, and J. Faist, Science **327**, 1495 (2010).
3. L. He, S. K. Özdemir, and L. Yang, Laser Photon. Rev. **7**, 60 (2013).
4. S. K. Tang, R. Derda, Q. Quan, M. Lončar, and G. M. Whitesides, Opt. Express **19**, 2204 (2011).
5. D. Bajoni, P. Senellart, E. Wertz, I. Sagnes, A. Miard, A. Lemaître, and J. Bloch, Phys. Rev. Lett. **100**, 047401 (2008).
6. Q. Gu, J. S. Smalley, M. P. Nezhad, A. Simic, J. H. Lee, M. Katz, O. Bondarenko, B. Slutsky, A. Mizrahi, V. Lomakin, and Y. Fainman, Adv. Opt. Photon. **6**, 1 (2014).
7. Z. Y. Li and D. Psaltis, Microfluid. Nanofluid. **4**, 145 (2008).
8. B. Ellis, M. A. Mayer, G. Shambat, T. Sarmiento, J. Harris, E. E. Haller, and J. Vučković, Nat. Photonics **5**, 297 (2011).
9. S. Matsuo, A. Shinya, T. Kakitsuka, K. Nozaki, T. Segawa, T. Sato, Y. Kawaguchi, and M. Notomi, Nat. Photonics **4**, 648 (2010).
10. A. Kiraz, Q. Chen, and X. Fan, ACS Photon. **2**, 707 (2015).
11. M. Nomura, S. Iwamoto, N. Kumagai, and Y. Arakawa, Phys. Rev. B **75**, 195313 (2007).
12. H. Yokoyama and S. D. Broson, J. Appl. Phys. **66**, 4801 (1989).
13. C. Karnutsch, Appl. Phys. Lett. **90**, 131104 (2007).
14. C. Dang, J. Lee, C. Breen, J. S. Steckel, S. Coe-Sullivan, and A. Nurmikko, Nat. Nanotechnol. **7**, 335 (2012).
15. S. Wu, S. Buckley, J. R. Schaibley, L. Feng, J. Yan, D. G. Mandrus, F. Hatima, W. Yao, J. Vučković, A. Majumdar, and X. Xu, Nature **520**, 69 (2015).
16. T. K. Fryett, K. L. Seyler, J. Zheng, C. Liu, X. Xu, and A. Majumdar, 2D Mater. **4**, 015031 (2017).
17. T. C. Lu, C. C. Kao, H. C. Kuo, G. S. Huang, and S. C. Wang, Appl. Phys. Lett. **92**, 141102 (2008).
18. M. Brune, F. Schmidt-Kaler, A. Maali, J. Dreyer, E. Hagley, J. M. Raimond, and S. Haroche, Phys. Rev. Lett. **76**, 1800 (1996).
19. S. Zhu, H. Dai, B. Jiang, Z. Shen, and X. Chen, Phys. Chem. Chem. Phys. **18**, 4585 (2016).
20. P. Andrew and W. L. Barnes, Science **306**, 1002 (2004).
21. Y. Zheng, Z. Cao, and X. Chen, J. Opt. Soc. Am. A **30**, 1901 (2013).
22. W. Yuan, C. Yin, P. Xiao, X. Wang, J. Sun, S. Huang, X. Chen, and Z. Cao, Microfluid. Nanofluid. **11**, 781 (2011).